Measurements on the Flow of Vapors near Saturation Through Porous Vycor Glass Membranes

Thomas Loimer[*], Jirina Reznickova[†], Petr Uchytil[†] and Katerina Setnickova[†]

[*]*Institute of Fluid Mechanics and Heat Transfer, Vienna University of Technology, Resselgasse 3, 1040 Wien, Austria*

[†]*Institute of Chemical Process Fundamentals of the Academy of Sciences of the Czech Republic, Rozvojova 2/135, 16502 Prague 6, Czech Republic*

Abstract.

We present experimental data of the flow of butane and isobutane vapors through porous Vycor glass membranes. The pressure driven flow of vapors near and far from saturation through membranes with pore diameters of 20 and 33 nm is investigated. The upstream pressures lie between the saturation pressure at the upstream temperature to approximately half that value. The pressure differences are between a few kPa to about 100 kPa.

From an adiabatic description of the flow process, we expect condensation of a vapor close enough to saturation and hence, due to the action of capillary forces, an increase in mass flux with respect to the mass flux of a vapor that remains in a gaseous state. According to the adiabatic description, a vapor that flows through a porous membrane may condense for two reason: One reason is capillary condensation in the pores of the membrane, the second reason is heat conduction from the upstream to the downstream side of the membrane due to the Joule-Thomson effect. If the flux of heat in downstream direction is large enough, a vapor near saturation at the upstream side of the membrane may only release sufficient heat by condensation.

Describing the flow in terms of dimensionless groups recovered from an adiabatic description of the flow process, we find that a vapor condenses and the mass flux is increased if (i) a dimensionless permeability of the membrane is larger than one and (ii) if the vapor at the upstream side is close enough to saturation such that a dimensionless group involving the upstream pressure and the pressure difference is also larger than one. Experimental data corroborates condition (i) above and indicates that condition (ii) might be valid.

Keywords: inorganic membranes, Joule-Thomson process, condensation, evaporation
PACS: 47.56.+r, 68.03.Fg

INTRODUCTION

We theoretically and experimentally investigate the flow of vapors through porous Vycor glass membranes. The mass flow of butane and isobutane vapors through Vycor glass membranes with pore diameters between 20 nm and 200 nm is measured. The membranes have the shape of a circular plate with a diameter of around 20 mm and a thickness between 0.5 and 1 mm. Due to the geometrical configuration, the flow can be considered as one-dimensional.

For vapors in a state near or at saturation upstreams of the membrane, condensation of the vapor is expected. The vapor can condense for two reasons: One reason is capillary condensation within the pores of the membrane [1], the second reason for condensation is the Joule-Thomson effect of real gases: The adiabatic, one-dimensional flow of a vapor through a porous medium of small permeability constitutes an adiabatic throttling process. Due to the Joule-Thomson effect, the fluid is cooler at the downstream side of the membrane than at the upstream side. The negative temperature gradient causes the transport of heat in downstream direction. A vapor far from saturation may release heat by a decrease in temperature, but a vapor at saturation can only release heat by condensation. Hence, regardless of the wetting properties between the solid matrix of the membrane and the fluid, due to the Joule-Thomson effect a vapor that flows through a porous membrane may condense [2].

The adiabatic flow of vapors through porous media was investigated by several authors [1, 3, 4]. Rhim and Hwang [1] observed that the enthalpy of vaporization released or consumed in phase changes makes the process non-isothermal, even if the fluid is kept at the same temperature at the upstream and the downstream station. Also, in a different context, Tien had stated, referring to the flow of a vapor through a porous medium [5, p. 170], “Another basic thermodynamic phenomenon that may play an interesting role in heat-pipe performance under certain conditions has never been mentioned or analyzed in the literature. This is the Joule-Thomson effect of real-gas flow.”

NOMENCLATURE

h	specific enthalpy (J/kg)
k	thermal conductivity (J/mK)
K	dimensionless permeability, see Eq. (8)
L	membrane thickness (m)
n	dimensionless fluid property, see Eq. (9)
p	pressure (Pa)
P_1	dimensionless group, see Eq. (11)
$\dot{q}$	heat flux (W/m^2)
r	pore radius (m)
R	specific gas constant (J/kgK)
T	temperature (K)
z	coordinate (m)

Greek Symbols

κ	permeability (m^2)
ν	kinematic viscosity (m^2/s)
Π	dimensionless pressure difference, see Eq. (10)
σ	surface tension (N/m)

Subscripts

g	gaseous
K	equilibrium properties at a curved interface
l	liquid
m	solid matrix
sat	properties at saturation

However, later the pressure-driven flow of vapors near saturation through porous Vycor glass or other inorganic membranes was mostly described as an isothermal process [3, 4, 6–8]. Lee and Hwang [3] or Abeles et al. [4] measured the flow of vapors through glass membranes with pore diameters of at most 6 nm [4], while Uhlhorn et al. [6] used alumina membranes with a pore diameter of 3 nm. As is appropriate for these pore sizes, apart from capillary forces, these authors also took account of effects caused by molecular forces between the fluid and the solid medium, e.g., adhesion and surface diffusion. Sidhu and Cussler [7] measured the flow of nitrogen under cryogenic conditions through track-etched polycarbonate membranes with a pore diameter of 10 nm. They observed a 50-fold increase in the mass flow under certain conditions and explained this increase with capillary condensation. They assumed isothermal flow, but did not account for molecular interaction forces. In the description of the flow presented here, molecular interaction forces are not considered, hence the description of the flow is restricted to media with pore sizes larger than around 10 nm.

Schneider [2] investigated the flow of isobutane through a stretched polypropylene membrane with a pore width of around 50 nm. He took account of the energy balance and of heat conduction and found that, even not considering capillary effects, due to the Joule-Thomson effect a saturated vapor may condense. He derived an expression for a characteristic permeability of the membrane and proposed that for a permeability of the membrane smaller than the characteristic permeability a saturated vapor condenses completely, while it condenses partially for a permeability of the membrane larger than the characteristic permeability. For full condensation, the mass flux is increased due to the large difference between the kinematic viscosities of the liquid and the vapor phase of the fluid.

Loimer [9] extended the description of Schneider [2] by accounting for capillary pressure and for vapor pressure reduction at curved interfaces. Thus, in a way, Loimer [9] combined isothermal [3, 4, 6–8] and adiabatic [2] descriptions. Later, the flow of saturated and unsaturated vapors was computed numerically and compared to experimental data [10]. Loimer et al. found that by accounting for capillary effects the expression for the characteristic permeability proposed by Schneider had to be modified. The experimental data reported by Loimer et al. [10] corroborated the importance of the characteristic permeability with respect to condensation.

THEORY

The flow process is described by modeling the porous medium as a bundle of equivalent capillaries. Darcy's law is assumed to be valid within the porous medium, and the pressure differences between the liquid and the vapor phase within the porous medium are given by the Young-Laplace equation, based on the radius of the effective capillaries. Hence, the balances of mass, momentum and energy are given by

$$\dot{m} = \text{constant}, \tag{1}$$

$$\dot{m} = -\frac{\kappa}{\nu}\frac{\mathrm{d}p}{\mathrm{d}z}, \tag{2}$$

$$\dot{m}h + \dot{q} = \text{constant}, \tag{3}$$

where $\dot{m}$ is the mass flux, κ denotes the permeability of the porous medium, ν refers to the kinematic viscosity of the fluid, h to the specific enthalpy of the fluid, p is the pressure and z is the coordinate in flow direction. The

heat flux is given by

$$\dot{q} = -k\frac{\mathrm{d}T}{\mathrm{d}z}, \tag{4}$$

where k refers to the effective thermal conductivity of the fluid-filled porous medium and T is the temperature.

At fronts of phase change within the porous medium, the vapor pressure is p_K, which is given by Kelvin's equation,

$$\ln\left(\frac{p_\mathrm{K}}{p_\mathrm{sat}}\right) = -\frac{2\sigma\cos\theta}{r}\frac{v_\mathrm{l}}{RT}, \tag{5}$$

where p_sat is the saturation pressure, the surface tension is given by σ, θ is the contact angle and r refers to the pore radius. The specific volume of the liquid is given by v_l and R is the specific gas constant.

The governing equations are solved subject to the boundary conditions

$$T = T_1,\ p = p_1,\ \dot{q} = 0 \quad \text{at } z \to -\infty, \tag{6}$$

$$p = p_2 \quad \text{at } z = L, \tag{7}$$

where L is the length of the membrane and the restriction $p_1 \le p_\mathrm{sat}$ applies. Further details of the theoretical description are given in Ref. [10].

The flow process is characterized by four dimensionless quantities, a permeability K,

$$K = \frac{\kappa\Delta h_\mathrm{vap,K}(\mathrm{d}p_\mathrm{K}/\mathrm{d}T - (2\cos\theta/r)(\mathrm{d}\sigma/\mathrm{d}T))}{v_\mathrm{l}k_\mathrm{m,l}}, \tag{8}$$

where $\Delta h_\mathrm{vap,K}$ is the enthalpy of vaporization at a curved interface and $k_\mathrm{m,l}$ refers to the thermal conductivity of the porous medium filled with the liquid phase of the fluid. The remaining dimensionless quantities are a fluid property n, a pressure difference Π and a upstream pressure P_1 which also involves the applied pressure difference,

$$n = \left(\frac{\partial T}{\partial p}\right)_h\left(\frac{\mathrm{d}p_\mathrm{K}}{\mathrm{d}T}\right), \tag{9}$$

$$\Pi = \frac{(p_1 - p_2)(1-n)}{p_\mathrm{sat} - p_\mathrm{K}}, \tag{10}$$

$$P_1 = \frac{p_1 - p_\mathrm{K} + n(p_1 - p_2)}{p_\mathrm{sat} - p_\mathrm{K} + n(p_1 - p_2)}. \tag{11}$$

The dimensionless permeability K results from evaluating the energy equation at the upstream front of the membrane for the marginal case that the vapor just condenses completely,

$$\dot{m}\Delta h_\mathrm{vap,K} = -k\frac{\mathrm{d}T}{\mathrm{d}z}. \tag{12}$$

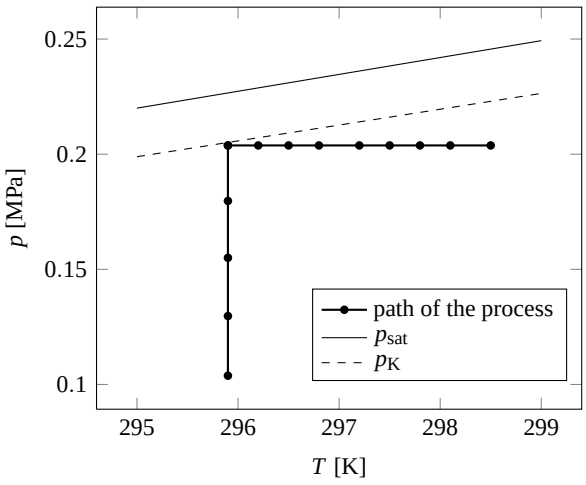

FIGURE 1. Path of a vapor in a p-T diagram for $P_1 = 0$. Flow of butane through a porous Vycor glass membrane, $T_1 = 298.45$ K, $p_1 - p_2 = 0.1$ MPa.

Substituting for $\dot{m}$ from Eq. (2) and assuming a pressure gradient such that the condensate, on permeating downstreams, just stays in equilibrium with its vapor state,

$$\frac{\mathrm{d}p}{\mathrm{d}z} = \frac{\mathrm{d}(p_\mathrm{K} - 2\sigma\cos\theta/r)}{\mathrm{d}T}\frac{\mathrm{d}T}{\mathrm{d}z}, \tag{13}$$

yields a characteristic permeability of the membrane or, alternatively, the definition of K ensues. Hence, a vapor that flows through a porous membrane with a permeability $K > 1$ condenses partially and a two-phase mixture flows through a part of the membrane, while a vapor that flows through a membrane with a permeability $K < 1$ condenses completely and liquid flows through a part of the membrane.

Whether the vapor condenses completely or partially bears important consequences on the mass flow through the membrane. For complete condensation, due to capillary action the mass flux is greatly enhanced with respect to the mass flux of a vapor that stays in its gaseous phase, while for partial condensation, there is only little increase of the mass flux. At a difference, assuming isothermal flow, complete condensation and an increase of the mass flux occurs whenever $p_1 > p_\mathrm{K}$, regardless of the permeability of the membrane.

The definition of P_1 can be inferred from the p-T diagram of a vapor that undergoes a throttling process. Figure 1 shows the path of a vapor that is in a state at the upstream side of the membrane such that condensation just does not occur, i.e., $p_1 = p_\mathrm{K} - n(p_1 - p_2)$. Whence, the definition of P_1 follows. As can be seen from Fig. 1, the temperature of the vapor is decreased isobarically in front of the membrane, while in the membrane the pressure is nearly isothermically decreased.

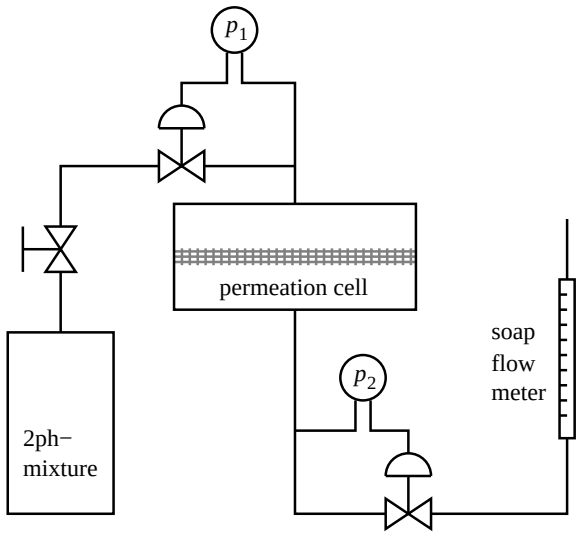

FIGURE 2. Experimental setup.

MEASUREMENTS

Experiments were performed by measuring the mass flow of butane and isobutane vapors through various Vycor glass membranes. The experimental setup is sketched in Fig. 2. The membranes were mounted in a permeation cell. A bottle containing a two-phase mixture of the fluid was connected via a pressure regulation valve to the upstream side of the permeation cell. Since the tubing was connected to the top of the bottle, saturated vapor was withdrawn from the bottle. From the downstream side of the permeation cell the vapor was led to a second pressure regulation valve and further downstreams to a soap flow meter, from where it exhausted to the atmosphere. From the volume flow readings and knowing the atmospheric conditions, the mass flow rate could be calculated. In addition, thermocouples were located at the upstream and the downstream side of the permeation cell, to measure the temperature or the temperature difference.

The mass flow is made dimensionless with the mass flux that is expected if the vapor remains in a gaseous state,

$$\dot{m}_\mathrm{g} = \frac{\kappa}{\nu_\mathrm{app}} \frac{p_1 - p_2}{L}. \tag{14}$$

Here, account is taken of the contribution of free molecular flow to viscous flow by using an apparent kinematic viscosity ν_app for the vapor [9].

A vapor close to saturation condenses and due to capillary action the mass flux is increased with respect to $\dot{m}_\mathrm{g}$. According to the adiabatic description [9, 10], a vapor condenses if $P_1 > 0$, i.e., $p_1 > p_\mathrm{K} - n(p_1 - p_2)$, while according to isothermal descriptions [3, 4, 6, 7] a vapor condenses if $p_1 > p_\mathrm{K}$. Figure 3 shows measured mass fluxes versus P_1 and versus $p_1 - p_\mathrm{K}$, normalized with $p_\mathrm{sat} - p_\mathrm{K}$. Measurements for membranes with pore diameters of 20 nm and of 33 nm are shown. The two graphs in Fig. 3 seem to give the indication that $\dot{m}/\dot{m}_\mathrm{g}$ is indeed larger than 1 for $P_1 > 0$, not for $p_1 > p_\mathrm{K}$. However, there is only one data point which truly supports this cause, an asterisk located at $\dot{m}/\dot{m}_\mathrm{g} \approx 1.3$ and $P_1 \approx 0.5$ on the left side and at $(p_1 - p_\mathrm{K})/(p_\mathrm{sat} - p_\mathrm{K}) \approx -0.5$ on the right side.

Moreover, in Fig. 3 a line shows the mass flow calculated from the adiabatic description [10] for one of the two cases and for a pressure difference of 50 kPa. Since for $P_1 > 1$ the ratio $\dot{m}/\dot{m}_\mathrm{g}$ depends on the pressure difference and the data depicted in Fig. 3 was taken over a range of pressure differences, the line shown in Fig. 3 can not be directly compared to the experimental data. Nevertheless, the measured mass fluxes are much smaller than the predicted values. For $p_1 = p_\mathrm{sat}$ a value of $\dot{m}/\dot{m}_\mathrm{g} = 8.7$ is calculated, while the maximum of the measured data is at about 4. However, assuming an isothermal flow and accounting for the capillary pressure, a value of $\dot{m}/\dot{m}_\mathrm{g} = 31$ is calculated.

Figure 3 shows that there is a huge scatter of the experimental data at $p_1 \approx p_\mathrm{sat}$. The scatter is mainly due to different applied pressure differences for each data point, see Fig. 4.

Figure 4 shows plots of the normalized mass flux versus dimensionless and versus dimensional pressure difference, respectively. The measured values have a nearly constant level of normalized mass fluxes for pressure differences between about 20 and 50 kPa. If the pressure difference is scaled with Π, these plateaus shift to different locations for the two data sets. Hence, the scaling with Π does not seem to be correct. The agreement between the calculated and the measured data is better for large pressure differences, but for small pressure differences, the agreement is poor. For pressure differences larger than 50 kPa, the decrease of $\dot{m}/\dot{m}_\mathrm{g}$ with increasing pressure difference is qualitatively reproduced.

CONCLUSIONS

Data on the mass flux of butane and isobutane vapors through porous Vycor glass with pore diameters of 20 and 33 nm is reported. The mass flux of vapors close to saturation is increased with respect to the mass flux of a vapor that remains in a gaseous state only if the dimensionless permeability of the membrane K, cf. Eq. (8), is larger than 1 [7, 10].

The data presented here indicates that a vapor is close enough to saturation for an increase in mass flux to occur if the upstream pressure is larger than $p_\mathrm{K} - n(p_1 - p_2)$. However, there is not enough data to conclusively answer the question whether the correct criterion is $p_1 > p_\mathrm{K} - n(p_1 - p_2)$ or $p_1 > p_\mathrm{K}$.

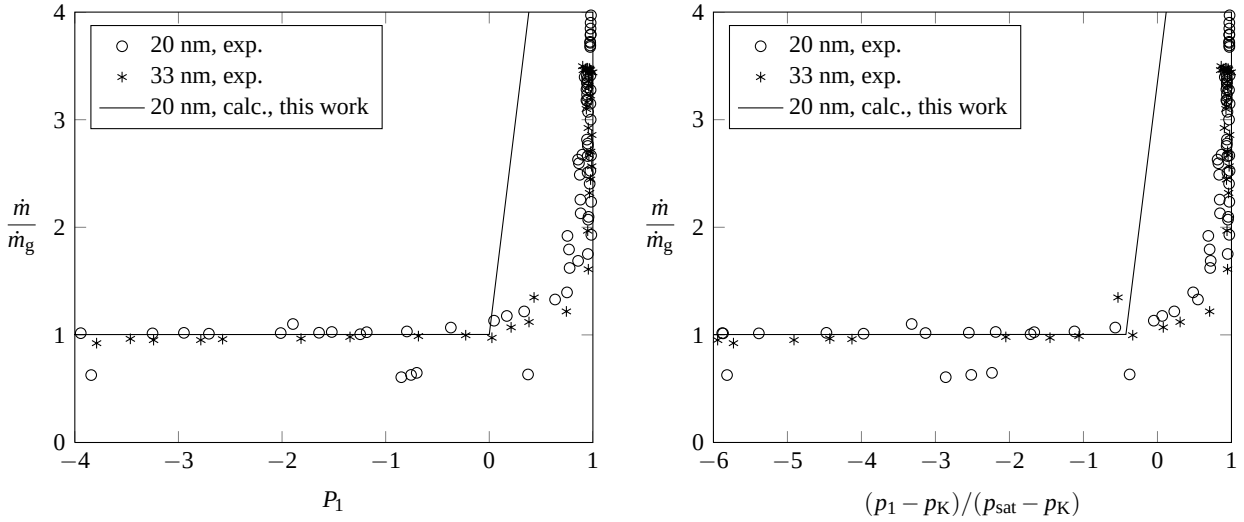

FIGURE 3. Mass flux versus P_1 (left) and versus $(p_1 - p_K)/(p_{sat} - p_K)$ (right). Data for the flow of butane, $T_1 = 25,3\,^\circ$C, through a membrane with pore diameter 20 nm and for the flow of isobutane, $T_1 = 24,2\,^\circ$C, pore diameter 33 nm, respectively. The solid line shows the mass flux calculated according to the adiabatic description [10] for $p_1 - p_2 = 50$ kPa.

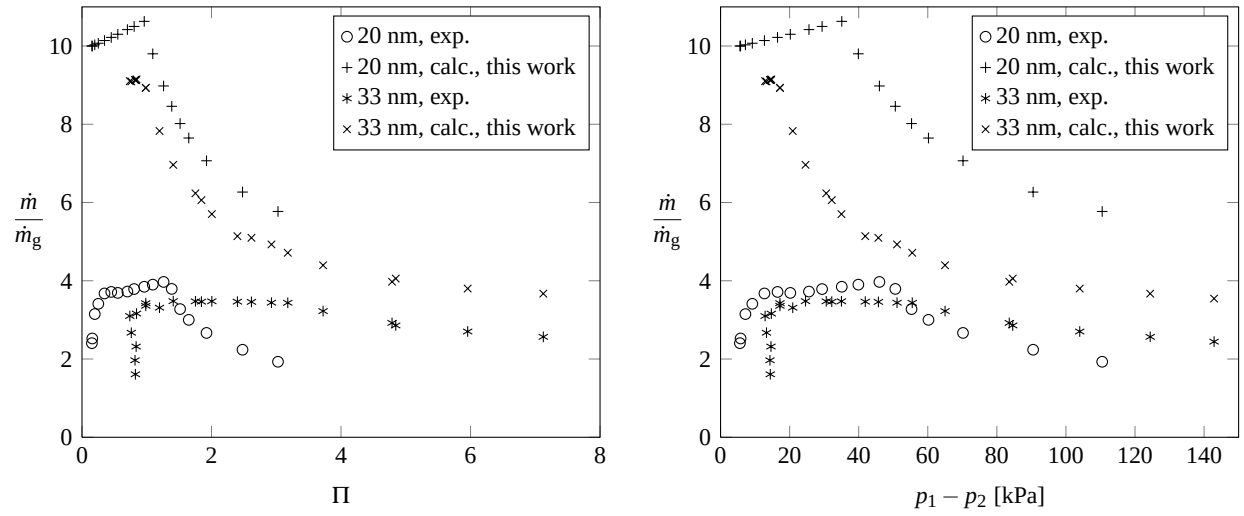

FIGURE 4. Mass flux versus dimensionless pressure difference (left) and versus pressure difference (right). Plotted here is the part of the data shown in Fig. 3 for which $P_1 > 0.9$ (20 nm) or for which $P_1 > 0.96$ (33 nm).

For pressure differences smaller than about 20 kPa, the mass flux data shows considerable scatter.

Qualitatively, the mass fluxes are much smaller than expected from an adiabatic or from isothermal descriptions of the flow, in which a constant contact angle is assumed and molecular interactions between the porous matrix and the fluid, e.g., adhesion, are not taken into account.

ACKNOWLEDGMENTS

Financial support by Androsch International Management Consulting GmbH, by the Austrian Exchange Service, grant no. CZ 08/2012 and by the Ministry of Education, Youth and Sports of the Czech Republic, grant 7AMB12AT009, is greatly acknowledged.

REFERENCES

1. H. Rhim, and S.-T. Hwang, *J. Colloid Interface Sci.* **52**, 174–181 (1975).
2. W. Schneider, *Acta Mech.* **47**, 15–25 (1983).
3. K.-H. Lee, and S.-T. Hwang, *J. Colloid Interface Sci.* **110**, 544–555 (1986).
4. B. Abeles, L.-F. Chen, J. W. Johnson, and J. M. Drake, *Isr. J. Chem.* **31**, 99–106 (1991).
5. C. L. Tien, *Ann. Rev. Fluid Mech.* **7**, 167–185 (1975).
6. R. J. R. Uhlhorn, K. Keizer, and A. J. Burggraaf, *J. Membr. Sci.* **66**, 259–269 (1992).
7. P. S. Sidhu, and E. L. Cussler, *J. Membr. Sci.* **182**, 91–101 (2001).
8. P. Uchytil, R. Petrickovic, S. Thomas, and A. Seidel-Morgenstern, *Sep. Purif. Technol.* **33**, 273–281 (2003).
9. T. Loimer, *J. Membr. Sci.* **301**, 107–117 (2007).
10. T. Loimer, P. Uchytil, R. Petrickovic, and K. Setnickova, *J. Membr. Sci.* **383**, 104–115 (2011).